Geometry optimization of a barrel silicon pixelated tracker [*]

Qing-Yuan Liu(刘清源)[1,2]   Meng Wang(王萌)[1;1)]   Marc Winter[2]

[1] School of Physics and Key Laboratory of Particle Physics and Particle Irradiation (MOE), Shandong University, Jinan 250100, China
[2] Université de Strasbourg, IPHC-CNRS, 23 rue du Loess, 67037 Strasbourg, France

Abstract: We have studied optimization of the design of a barrel-shaped pixelated tracker for given spatial boundaries. The optimization includes choice of number of layers and layer spacing. Focusing on tracking performance only, momentum resolution is chosen as the figure of merit. The layer spacing is studied based on Gluckstern's method and a numerical geometry scan of all possible tracker layouts. A formula to give the optimal geometry for curvature measurement is derived in the case of negligible multiple scattering to deal with trajectories of very high momentum particles. The result is validated by a numerical scan method, which could also be implemented with any track fitting algorithm involving material effects, to search for the optimal layer spacing and to determine the total number of layers for the momentum range of interest under the same magnetic field. The geometry optimization of an inner silicon pixel tracker proposed for BESIII is also studied by using a numerical scan and these results are compared with Geant4-based simulations.

Keywords: tracker geometry optimization, optimal spacing, numerical scan, least squares, kalman filter initialization, BESIII silicon pixel tracker

PACS: 07.05.Fb, 07.05.Tp   **DOI:** 10.1088/1674-1137/41/8/086001

1 Introduction

Silicon pixel detectors have been widely used in high energy physics experiments due to their excellent spatial resolution, high readout speed, great radiation hardness and acceptable material budget. Although their most important role is as vertex detectors, there is a trend to use them as tracking detectors, in conjunction with traditional gaseous detectors, or even on their own. For instance, the ALICE experiment has decided to upgrade its Inner Tracking System based on monolithic CMOS pixel detectors [1]; the BESIII experiment has been carrying out R&D on replacing its inner drift chamber with a CMOS pixel sensor (CPS)-based detector [2]; and for future experiments such as the Circular Electron Position Collider (CEPC), pixelated trackers are also foreseen.

In addition to the advantages mentioned above, a pixel tracker could have their thin solid layers placed with different spacings to achieve better curvature resolution than gas trackers, which are constructed with uniform spacing. As the total number of layers N in a silicon system is much smaller than that of the sensing layers in gas chambers, the optimal spacing proposed by Gluckstern [3] and Karimäki [4] may not be suitable for some particular values of N. Furthermore, a tracker should be designed to be sensitive to the transverse mo-

mentum of typical final state particles. This requires an optimization of the layer configuration which considers multiple scattering. Since an analytical solution is too complex, a numerical scan of the geometries will allow finding of the tracker layout with the optimal curvature resolution. Although a related Java software based on extended Kalman filters (EKF) was developed in 2008 [5], it does not include the case of several layers placed around one position.

The geometry or spacing of a bubble tracker was studied by Gluckstern in the 1960s using weighted least squares and a parabola approximation to estimate the covariances of the trajectory direction and curvature [3]. The optimal spacing for track curvature measurement without multiple scattering effects was given with $N/2$ measurements taken at the centre of the tracker and the other half measured at both ends of the detecting region equally, that is the layer configuration $N/4-N/2-N/4$ at positions $x = 0, L/2, L$ where L is the length of the tracker lever arm in a telescope system or the radial distance from the innermost layer to the outermost in cylindrical trackers. In the 1990s, Karimäki developed explicit formulae to calculate the parameter covariances of circle tracks using a non-linear extension of the least squares method [4, 6]. The spacing to achieve the best curvature accuracy in Karimäki's strategy is the same

as Gluckstern's when N is a multiple of 4. In addition, Karimäki pointed out that the measurements should be taken symmetrically with respect to the centre of the tracker and maximize the product $M(N-M)$, in which M is the number of measurements at $x=L/2$.

Compared with the circle model in Karimäki's nonlinear least squares calculation, the parabola approximation leads to an overestimated curvature variance by a factor about $(L/R)^2/21$[1], where R is the radius of the trajectory [4]. Nevertheless, this overestimation is close to 0 in the case where the trajectory has sufficient projected momentum high enough in the bending plane to neglect multiple scattering. Therefore, the optimal spacing for very high momentum tracks could be studied by the convenient parabola approximation because of extremely small $(L/R)^2$.

In this article, the optimal spacing (only considering measurement errors) is studied by using the linear least squares method on trajectories in the bending plane, and the strategy of a geometry scan will be defined to determine the total number of layers and the best layer configuration for a given momentum, ladder design, magnetic field and intrinsic spatial resolution of each layer. In Section 2, a new formula is proposed to get the optimal spacing for $N \geqslant 3$ without the constraint of having the same number of measurements at both ends of a tracker in the case of neglecting the multiple scattering. In Section 3, the geometry optimization with multiple scattering based on a combination recursion tree and track parameter variances calculation is introduced. The conditions to choose a proper track fitting algorithm are also given. In Section 4, the optimization of the inner silicon pixel tracker designed for BESIII is provided and the results are compared with full Monte Carlo simulations.

2 Curvature variance and optimal spacing without multiple scattering

2.1 Variance equations of the tracking system

We start from the parabola equation below:

$$y=a+bx+cx^2,$$

in which y is the measurement at x, parameter a is the intercept at $x=0$, b is the track direction and c is equal to $1/(2R)$, half of the track curvature at $x=0$. In the case of no multiple scattering, the generalized least squares will be simplified to the weighted least squares and the variance matrix of the parameters is given below:

$$
\boldsymbol{V_{\hat{\theta}}} =
\begin{bmatrix}
\sum_{j=1}^{N} 1/\sigma_j^2 & \sum_{j=1}^{N} x_j/\sigma_j^2 & \sum_{j=1}^{N} x_j^2/\sigma_j^2 \\
\sum_{j=1}^{N} x_j/\sigma_j^2 & \sum_{j=1}^{N} x_j^2/\sigma_j^2 & \sum_{j=1}^{N} x_j^3/\sigma_j^2 \\
\sum_{j=1}^{N} x_j^2/\sigma_j^2 & \sum_{j=1}^{N} x_j^3/\sigma_j^2 & \sum_{j=1}^{N} x_j^4/\sigma_j^2
\end{bmatrix}^{-1} , \quad (1)
$$

where $\hat{\boldsymbol{\theta}}$ is the vector of the three estimated parameters defined by $\hat{\boldsymbol{\theta}}=(a,b,c)^T$ and σ_j is the measurement error of the j'th layer located at position x_j. To deal with the inversion in this equation and simplify the derivation, all the layers are supposed to have the same spatial resolution σ and the notation $X^{(k)}$ is introduced as follows:

$$X^{(k)} = \sum_{j=1}^{N} x_j^k, \qquad (2)$$

in which $k = 0,\ 1,\ 2,\ 3,\ 4$ and $X^{(0)} = N$. The auxiliary matrix $\boldsymbol{A_V}$ including all the geometry information is defined as:

$$
\boldsymbol{A_V} \equiv
\begin{bmatrix}
N & X^{(1)} & X^{(2)} \\
X^{(1)} & X^{(2)} & X^{(3)} \\
X^{(2)} & X^{(3)} & X^{(4)}
\end{bmatrix}. \qquad (3)
$$

Therefore the covariance matrix could be simplified as

$$\boldsymbol{V_{\hat{\theta}}} = \sigma^2 \boldsymbol{A_V^{-1}}. \qquad (4)$$

Finally, the explicit expression of the upper-right elements in the symmetric matrix $\boldsymbol{V_{\hat{\theta}}}$ reads

$$
\boldsymbol{V_{\hat{\theta}}} = \frac{\sigma^2}{|\boldsymbol{A_V}|}
\begin{bmatrix}
X^{(2)}X^{(4)}-X^{(3)}X^{(3)} & X^{(2)}X^{(3)}-X^{(1)}X^{(4)} & X^{(1)}X^{(3)}-X^{(2)}X^{(2)} \\
 & NX^{(4)}-X^{(2)}X^{(2)} & X^{(1)}X^{(2)}-NX^{(3)} \\
 & & NX^{(2)}-X^{(1)}X^{(1)}
\end{bmatrix}, \qquad (5)
$$

where $|\boldsymbol{A_V}|$ is the determinant of matrix $\boldsymbol{A_V}$. It indicates that the track fitting performance is only determined by the intrinsic spatial resolution of the sensors and the spacing of the layers. Naturally, the geometry optimization to achieve the best curvature measurement is changed into the minimization of the curvature-

related variance $V_{\hat{\theta}_{33}}$ in the covariance matrix described by Eq. (5). This variance is defined as V_{cc}, with the explicit form:

$$V_{cc} \equiv V_{\hat{\theta}_{33}} = \sigma^2 \frac{NX^{(2)}-X^{(1)}X^{(1)}}{|\boldsymbol{A_V}|}. \qquad (6)$$

---

1) L is the length of the lever arm in Gluckstern's method, but it stands for track segment length in Karimäki's calculation. Therefore, the overestimated factor $(L/R)^2/21$ itself is only valid for small $(L/R)^2$

Its partial derivative with respect to the position of the k'th layer reads

$$\frac{\partial V_{cc}}{\partial x_k} = \sigma^2 \frac{Y_1 \cdot Y_2}{|\boldsymbol{A_V}|^2}, \tag{7}$$

in which

$$Y_1 = 2 \sum_{i=1}^{N} \sum_{j=1}^{N} [x_i(x_k-x_j)(x_k-x_i)(x_j-x_i)], \tag{8}$$

$$Y_2 = \sum_{i=1}^{N} \sum_{j=1}^{N} [x_j(2x_k-x_j)(x_j-x_i)]. \tag{9}$$

If the indices i and j are exchanged in Eq. (8) and Eq. (9), the values of Y_1 and Y_2 will not be changed, such that we have:

$$\begin{aligned} Y_1 &= \sum_{i=1}^{N} \sum_{j=1}^{N} [x_i(x_k-x_j)(x_k-x_i)(x_j-x_i) + \\ &\qquad x_j(x_k-x_j)(x_k-x_i)(x_i-x_j)] \\ &= \sum_{i=1}^{N} \sum_{j=1}^{N} [-(x_k-x_i)(x_k-x_j)(x_j-x_i)^2], \end{aligned} \tag{10}$$

$$\begin{aligned} Y_2 &= \sum_{i=1}^{N} \sum_{j=1}^{N} [x_j(2x_k-x_j)(x_j-x_i) + \\ &\qquad x_i(2x_k-x_i)(x_i-x_j)] \cdot \frac{1}{2} \\ &= \sum_{i=1}^{N} \sum_{j=1}^{N} \left[(x_j-x_i)^2 (x_k - \frac{x_i+x_j}{2}) \right]. \end{aligned} \tag{11}$$

Usually, to minimize V_{cc} requires $\partial V_{cc}/\partial x_k = 0$ for all the layers, but this is not possible in our situation. The minimization can only be solved under certain constraints:

1) When $x_k = x_1$, x_k is the smallest value such that $Y_1 < 0$ and $Y_2 < 0$. The partial derivative

$$\frac{\partial V_{cc}}{\partial x_1} > 0,$$

therefore $V_{cc}(x_1)$ is an increasing function of x_1, which means x_1 should be as small as possible to obtain the smallest variance in track curvature. In practice, the position of the very first layer is limited by the beam pipe and background density in collider experiments.

2) When $x_k = x_N$, x_k is the position of the outermost layer in the tracker. $Y_1 < 0$ and $Y_2 > 0$ leads to

$$\frac{\partial V_{cc}}{\partial x_N} < 0,$$

such that V_{cc} is a decreasing function of x_N. To have smaller V_{cc}, x_N should be as large as possible. However, particles with low transverse momentum cannot reach layers which are too far away.

3) When $x_1 < x_k < x_N$, the layer to be studied is an intermediate one located between the innermost and the outermost. The formalization in Eq. (10) and Eq. (11) leads to a possible solution to this minimization problem. On condition of the same number of layers placed at x_1 and x_N, all the other layers should have the same position $x_k = (x_1+x_N)/2$. We have

$$\begin{aligned} \frac{\partial V_{cc}}{\partial x_k}\bigg|_{x_k = \frac{x_1+x_N}{2}} &= 0, \\ \frac{\partial V_{cc}}{\partial x_k}\bigg|_{x_k = \frac{x_1+x_N}{2}+\epsilon} &> 0, \\ \frac{\partial V_{cc}}{\partial x_k}\bigg|_{x_k = \frac{x_1+x_N}{2}-\epsilon} &< 0, \end{aligned}$$

in which $0 < \epsilon \ll (x_1+x_N)/4$.

Nevertheless, the optimization up to now does not answer the question of how many layers should be installed at x_1 and x_N. To find the optimal spacing overall, two positive fractions f_1 and f_2, which stand for the ratios of number of layers at $(x_1+x_N)/2$ over N and number of layers at x_N over N respectively, are introduced. $f_1+f_2 < 1$ should be guaranteed to have measurements at three different positions. Moreover, we can set $x_1 = 0$ and $x_N = L$, where L is the length of the lever arm of the tracker, without loss of generality. Therefore, the curvature variance V_{KK} can be derived from Eq. (6):

$$V_{KK} = 4V_{cc} = \frac{16\sigma^2}{NL^4} \left(\frac{4}{f_1} + \frac{1}{f_2} + \frac{1}{1-f_1-f_2} \right). \tag{12}$$

The minimization of V_{cc} with respect to f_1 and f_2 leads to $f_1 = 0.5$ and $f_2 = 0.25$, that is the same layer spacing configuration $N/4$–$N/2$–$N/4$ at beginning-center-end of the tracker as given by Refs. [3, 4].

In the case $f_2 = 1-f_1-f_2$, the numbers of measurements taken at the two ends of a tracker are equal. The curvature variance V_{KK} can be simplified as:

$$V_{KK} = \frac{64\sigma^2}{L^4} \frac{N}{Nf_1(N-Nf_1)}, \tag{13}$$

which is exactly the equation obtained by Karimäki [4]. Since Eq. (12) is more general, it should be used as long as the total number of layers $N \geq 3$.

When $f_2 \neq 1-f_1-f_2$, the number of measurements taken at $x=0$ and at $x=L$ are not equal, and the variance calculated by Eq. (12) is not optimal any more. The intuitive understanding is that the layers in the middle should be put closer to the tracker end with more measurements to balance the different weights from the two sides of the measured track segment. The optimal position for the middle layers can be found by solving for x_k

in the equation below:

$$2N(1-f_1-f_2)Nf_2L^2(x_k-\frac{L}{2})$$
$$+N(1-f_1-f_2)Nf_1x_k^3$$
$$+Nf_1Nf_2(x_k-L)^3=0. \tag{14}$$

2.2 Optimal spacing when N is not a multiple of 4

If the positions of the layers are always $x=0,L/2,L$, the optimal geometry which is described by f_1 and f_2 can be determined by minimizing V_{cc} in Eq. (12) in the definition domain[1] of the two fractions without the constraint of an equal number of layers at $x=0$ and $x=L$. The first optimal spacing which is unsymmetrical can be found at $N=6$. A comparison of the optimal[2] unsymmetrical spacing and symmetrical spacing is shown in Table 1, where the variances V_{aa}[3] and V_{bb}[4] are also calculated.

Although the unsymmetrical optimal spacing $2-3-1$ is only slightly better than the symmetrical one $2-2-2$ in terms of curvature variance, $2-3-1$ is the optimal when all track parameter variances are considered. By using Eq. (12), the geometries with the most accurate curvature measurement with a given number of layers $N\leq12$ are listed in Table 2.

Table 1.   Comparison of symmetrical optimal spacing and unsymmetrical spacing when $N=6$

spacing	V_{KK}	V_{aa}	V_{bb}
$2-3-1$	$272\sigma^2/NL^4$	$3\sigma^2/N$	$65\sigma^2/(NL^2)$
$1-3-2$	$272\sigma^2/NL^4$	$6\sigma^2/N$	$89\sigma^2/(NL^2)$
$1-4-1$	$288\sigma^2/NL^4$	$6\sigma^2/N$	$84\sigma^2/(NL^2)$
$2-2-2$	$288\sigma^2/NL^4$	$3\sigma^2/N$	$78\sigma^2/(NL^2)$

Table 2.   Optimal spacing for curvature measurement using N layers ($3\leqslant N\leqslant12$)

number of layers	configuration (begin-center-end)
3	$1-1-1$
4	$1-2-1$
5	$1-3-1$
6	$2-3-1$ or $1-3-2$
7	$2-3-2$
8	$2-4-2$
9	$2-5-2$
10	$3-5-2$ or $2-5-3$
11	$3-5-3$
12	$3-6-3$

In addition to this analytical method to optimize tracker geometry, numerical calculation with a scan of all possible spacing configurations is also possible to find the optimal layout. The advantage of an analytical solution is its very fast speed. However, it is difficult to include material effects such as multiple scattering which introduce correlations among the measurements and make the error matrix more complex.

3 Geometry optimization with multiple scattering

The method of geometry or layer spacing scan is inspired by Eq. (1), as the estimated track parameter variance is only a function of layer positions and their intrinsic spatial resolutions. Considering multiple scattering will only add contributions from the material budget of each layer into the parameter covariance matrix. This material contribution is a function of layer positions, layer thickness in units of radiation length, and momentum of the trajectory under a given magnetic field. To simplify the calculation and focus on the scan strategy itself, the study only involves tracks in the bending plane.

3.1 Spacing scan of N layers and its implementation

The innermost layer and the outermost are fixed at their positions $x_1=0$ and $x_N=L$. All the other layers can be moved by a user-specified step ΔL which satisfies the condition that $L/\Delta L$ is a multiple of $2(N-1)$ for even N or a multiple of $(N-1)$ for odd N to make sure that the position at the centre of the tracker and the uniform spacing configuration are possible. Once ΔL is chosen, the second layer should be placed at x_2, which ranges from x_1 to x_N, the third layer should be placed at x_3, whose range is from x_2 to x_N, and so on for the other unfixed layers. This process therefore requires N loops. Since we can change the total number of layers in a tracker, N is a variable, such that a recursive algorithm has to be used in the software. The possible positions $x=0,\Delta L,2\Delta L,...,L$ can be related to a series of numbers, that is $0,1,2,...,L/\Delta L$, thus all the geometries are changed into all the $(N-2)$-combinations of the number set.

As the optimal spacing could contain layers placed at the same position, repeated values in the number set are allowed. The number of levels in the recursion tree is equal to the number of unfixed layers. The simplest tree for 5 detecting layers is shown in Fig. 1. One may notice that the only combination of position-related numbers

---

1) Nf_1 and Nf_2 have to be integers

2) Optimization is only taken for minimizing the curvature variance given by Eq. (12). If Eq. (14) is used, the corrected position for all middle layers is around $0.46463L$ rather than $0.5L$ for the configuration $2-3-1$, and the variance improvement is smaller than 1.3%.

3) $V_{aa}=\frac{\sigma^2}{N}\frac{1}{1-f_1-f_2}$ when all the layers are placed only at positions $x=0,L/2,L$

4) $V_{bb}=\frac{\sigma^2}{NL^2}(\frac{16}{f_1}+\frac{1}{f_2}+\frac{9}{1-f_1-f_2})$
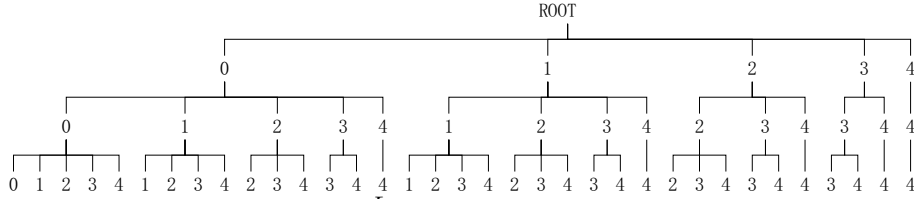
Fig. 1.   The recursion tree for $N=5$ and $\Delta L = \dfrac{L}{4}$. Only the position numbers of movable layers are shown. The index of the layer layout is counted from the left to the right of the tree. For instance, the first layout has the position set (0, 0,0,0, 4) while the last one has the set (0, 4,4,4, 4).

is (0,1,2,3,4) if no overlap of layers is required in this example.

3.2   Choice of a stable track fitting algorithm

After a tracker layout is determined from one combination of the recursion tree, the curvature variance can be calculated using a stable track fitting algorithm which satisfies the conditions below:

1) The pull distribution of track parameters should be a standard normal distribution for the momentum range of interest.

2) The above condition applies to all the tracker geometries in the scan.

To verify the two conditions above, a toy Monte Carlo simulation which only contains measurement uncertainties was used. By removing the influence of multiple scattering, the chosen tracking algorithm should work well in the relevant curvature or momentum range. In this study, a generalized least squares (GLS) fitting and an extended Kalman filter (EKF) are compared. The toy simulation consists in generating pions which traverse a 1 T magnetic field and are detected by three silicon ladders with 10 μm spatial resolution located at 72.58 mm, 86.16 mm and 99.50 mm from the origin.

The matrix notation below is used to define the parameter vector $\boldsymbol{\theta}$, the measurement vector $\boldsymbol{y}$ and the geometry matrix $\boldsymbol{A}$:

$$\boldsymbol{\theta} = \begin{bmatrix} a \\ b \\ c \end{bmatrix}, \quad \boldsymbol{y} = \begin{bmatrix} y_1 \\ \vdots \\ y_j \\ \vdots \\ y_N \end{bmatrix}, \quad \boldsymbol{A} = \begin{bmatrix} 1 & x_1 & x_1^2 \\ & \vdots & \\ 1 & x_j & x_j^2 \\ & \vdots & \\ 1 & x_N & x_N^2 \end{bmatrix},$$

χ^2 reads

$$\chi^2 = (\boldsymbol{y} - \boldsymbol{A\theta})^T \boldsymbol{V_y}^{-1} (\boldsymbol{y} - \boldsymbol{A\theta}), \qquad (15)$$

where $\boldsymbol{V_y}$ is the symmetric error matrix of $\boldsymbol{y}$ with the elements given below:

$$\boldsymbol{V_y}_{ij} = \sum_{l=1}^{i} (x_i - x_l)(x_j - x_l)\langle \delta\alpha_l \delta\alpha_l \rangle + \sigma_i^2 \delta_{ij}, \qquad (16)$$

in which $i \leqslant j (x_i \leqslant x_j)$, σ_i is the intrinsic spatial resolution

of the i'th layer and $\langle \delta\alpha_l \delta\alpha_l \rangle$ is the variance of multiple scattering angle at the l'th layer with its standard deviation given in Ref. [7]. In this simple implementation, the detecting layers are perpendicular to the x-coordinate, which works well for ladder sector designs.

The results of the toy simulation are shown in Fig. 2, where the bias of the parabola model can be seen for momenta below 0.3 GeV.
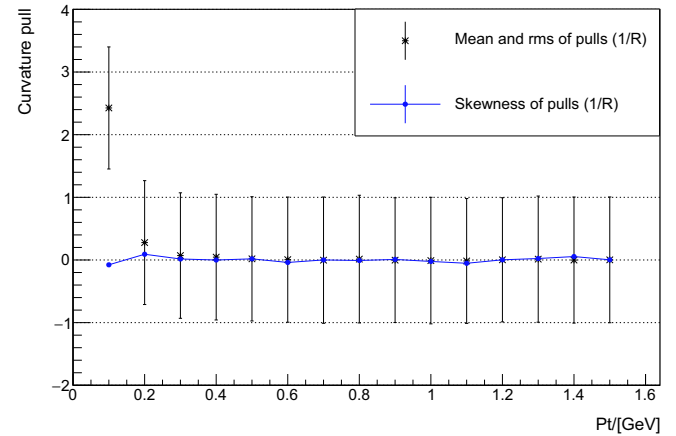
Fig. 2.   Curvature pulls vs momentum of GLS method. The pull of curvature is defined as $(k_{\mathrm{rec}} - k_{\mathrm{true}})/\sigma_k$ where σ_k is the estimated curvature deviation given by the fitting algorithm. Mean values and standard deviations of the curvature pulls are shown by black asterisks and error bars, and the skewness of the pull distribution and its error are marked in blue.

A similar plot was also drawn with the position of the second layer changed to 96.16 mm and no obvious difference was found. The features of the generalized least squares and Gluckstern's method are summarized below:

1) The curvature estimation has bias for low momentum trajectories, as $(L/R)^2$ is too large for the parabola approximation.

2) The estimation of curvature variance is always good for all the tested momenta.

3) Tracking performance is stable for different tracker structures.

As one of the alternatives, an inward tracking method based on EKF is also studied. As its initialization is re-

lated to the tracker layout as well as other possible tracking systems, it is not preferred in this geometry scan where thousands of layouts will be processed.

3.3 Geometry scan towards optimal spacing

The GLS algorithm is chosen to calculate track parameter variances for the geometry scan. The three-layer tracker in the previous toy simulation could be optimized very quickly. The optimal geometry is always three evenly placed layers regardless of multiple scattering. To verify the results in Section 2, a six-layer tracker in the same position range as that in the toy simulation was scanned, with the results shown in Fig. 3, with layer moving step $\sim$0.897 mm and with layer thickness set to zero.
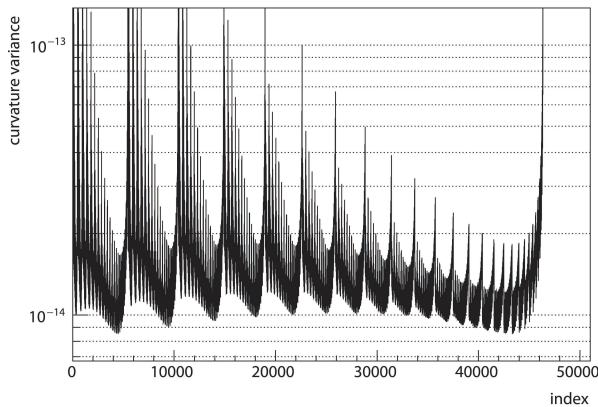
Fig. 3. The curvature variance (μm^{-2}) as a function of geometry indices in the same order of the recursion tree for $N=6$ and $\Delta L = \dfrac{L}{30}$.

The optimal configurations found from Fig. 3 are compared with uniform spacing in Table 3. Both the layouts and the corrected positions[1] of the middle layers coincide with the calculations in Section 2.

The same strategy involving multiple scattering can be processed by setting the correct layer thickness, and the application is introduced in Section 4.

Table 3. Results of the selected geometries.

index	configuration	middle position	$\sigma_K(p_{\mathrm{T}}=1$ GeV$)$
27601	uniform		0.113 m^{-1}
4487	2−3−1	85.143 mm	0.092 m^{-1}
43330	1−3−2	86.937 mm	0.092 m^{-1}

3.4 Choice of N, the total number of layers

Using the same spacing, Eq. (12) indicates that the curvature variance is proportional to $1/N$ for very high

momentum tracks. In this case, the larger N is the better, if financial budget is not a problem. However, this direct proportion is broken for relatively low momentum trajectories. Because of the rise of material effect, too many layers will smear the hits and make the tracking more inaccurate. To determine the number of layers, several values of N can be tried. By comparing the tracking performance of the optimal spacing for different N, the total number of layers and its related geometry can be determined at the same time.

4 Application to BESIII silicon pixel tracker

The silicon pixel tracker (SPT) is a proposal to replace the inner gas chamber of BESIII with CMOS pixel sensor ladders which have a spatial resolution around 10 μm and material budget $X/X_0 \sim 0.36\%$ [2]. The preliminary position range is from 72.58 mm to 99.50 mm. In our study, the GLS tracking described in Section 3 is used, so the ladders are simply placed perpendicular to the x-axis. Using the geometry scan of N layers where N is 3, 4 or 6, the layouts optimized for 0.3 GeV and 1.0 GeV trajectories with a fixed polar angle ($\theta = \pi/2$) are listed in Table 4.

Table 4. Optimized geometries for SPT.

N	P_{T}/GeV	step/mm	layer positions/mm
3	all	any	72.58, 86.04, 99.50
4	0.3	0.45	72.58, 72.58, 85.59, 99.50
4	1.0	0.45	72.58, 84.25, 87.83, 99.50
6	0.3	0.90	72.58, 72.58, 79.76, 92.32, 99.50, 99.50
6	1.0	0.90	72.58, 72.58, 84.25, 87.83, 99.50, 99.50

The momentum resolutions $\sigma_{p_{\mathrm{T}}}/p_{\mathrm{T}}$ calculated by GLS and the results from full Monte Carlo simulations are shown in Fig. 4. The predictions given by our strategy are in agreement with the simulated data. The momentum resolutions of all the geometries optimized for 0.3 GeV are similar and the 3-layer layout or the 4-layer one with uniform spacing are more favoured by tracks with the most probable momentum around 0.3 GeV. If the geometry is optimized for 1.0 GeV, the last geometry with 6 layers in Table 4 could be considered as the baseline design, which is $\sim$7% better than the uniform spacing.

5 Summary and discussion

A general strategy to optimize the design of a barrel pixelated tracker has been presented in this paper.

---

1) By using Eq. (14), the corrected position of layout 2−3−1 is 85.088 mm while that of layout 1−3−2 is 86.992 mm
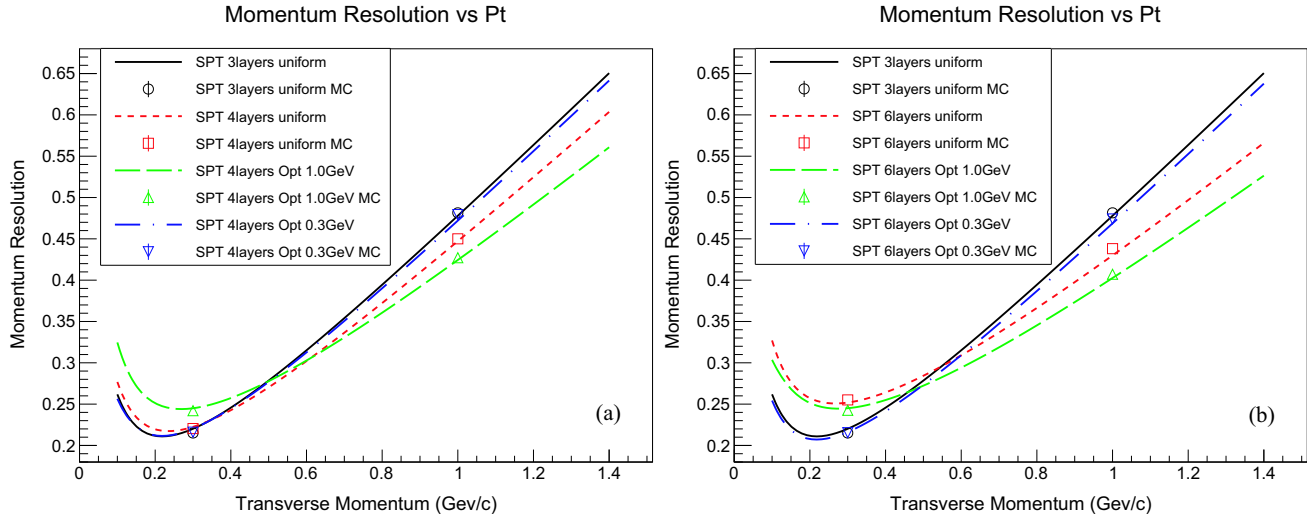
Fig. 4.   Comparison of relative momentum resolutions as a function of momentum of pions flying in the bending plane. (a) The resolutions for layouts with 3/4 layers. (b) The resolutions for layouts with 3/6 layers. The lines denote the predictions from GLS fitting of different geometries in which layer overlap is permitted, while the dots with error bars are used for MC results where the minimum layer interval is 1 mm.

Methods to search for the optimal spacing of N-layer silicon trackers with or without multiple scattering have been derived and verified by comparing the results of GLS tracking and the analysis of full Monte Carlo simulations in the simplified situation where trajectories are circle segments. For helical tracks, the corrections of the track length in material could be calculated from the azimuth and the polar angle to estimate multiple scattering more accurately. The requirements of tracking algorithms to be used in geometry scan have also been proposed. Since the numerical scan is compatible with the other tracking methods, the momentum range of the tracks could be extended and the energy loss effect could also be included by choosing a proper fitting algorithm. Finally, the total number of layers could also be determined by comparing the optimal spacing of different N in the geometry scan. Our methods have been applied to the inner silicon tracker design proposed for BESIII. As a general solution, applications to future detectors like CEPC can be foreseen, in which the geometry including the vertex detector should be optimized according to the momentum distributions of the final states of interest.

References

1 The ALICE Collaboration, J. Phys. G: Nucl. Part. Phys., **41**: 087002 (2014)
2 Q. Xiu et al, arXiv:1510.08558 [physics.ins-det].
3 R. L. Gluckstern, Nucl. Instrum. Methods, **24**: 381–389 (1963)
4 V. Karimäki, Nucl. Instrum. Methods, A, **410**: 284–292 (1998)
5 R. Frühwirth and A. Beringer, 2008 IEEE Nuclear Science Symposium Conference Record, 3483–3487 (2008)
6 V. Karimäki, Nucl. Instrum. Methods, A, **305**: 187–191 (1991)
7 G. R. Lynch and O. I. Dahl, Nucl. Instrum. Methods, B, **58**: 6–10 (1991)